eLIFE elifesciences.org

SHORT REPORT

Figures and figure supplements

Identification of a transporter complex responsible for the cytosolic entry of nitrogen-containing bisphosphonates

Zhou Yu *et al*

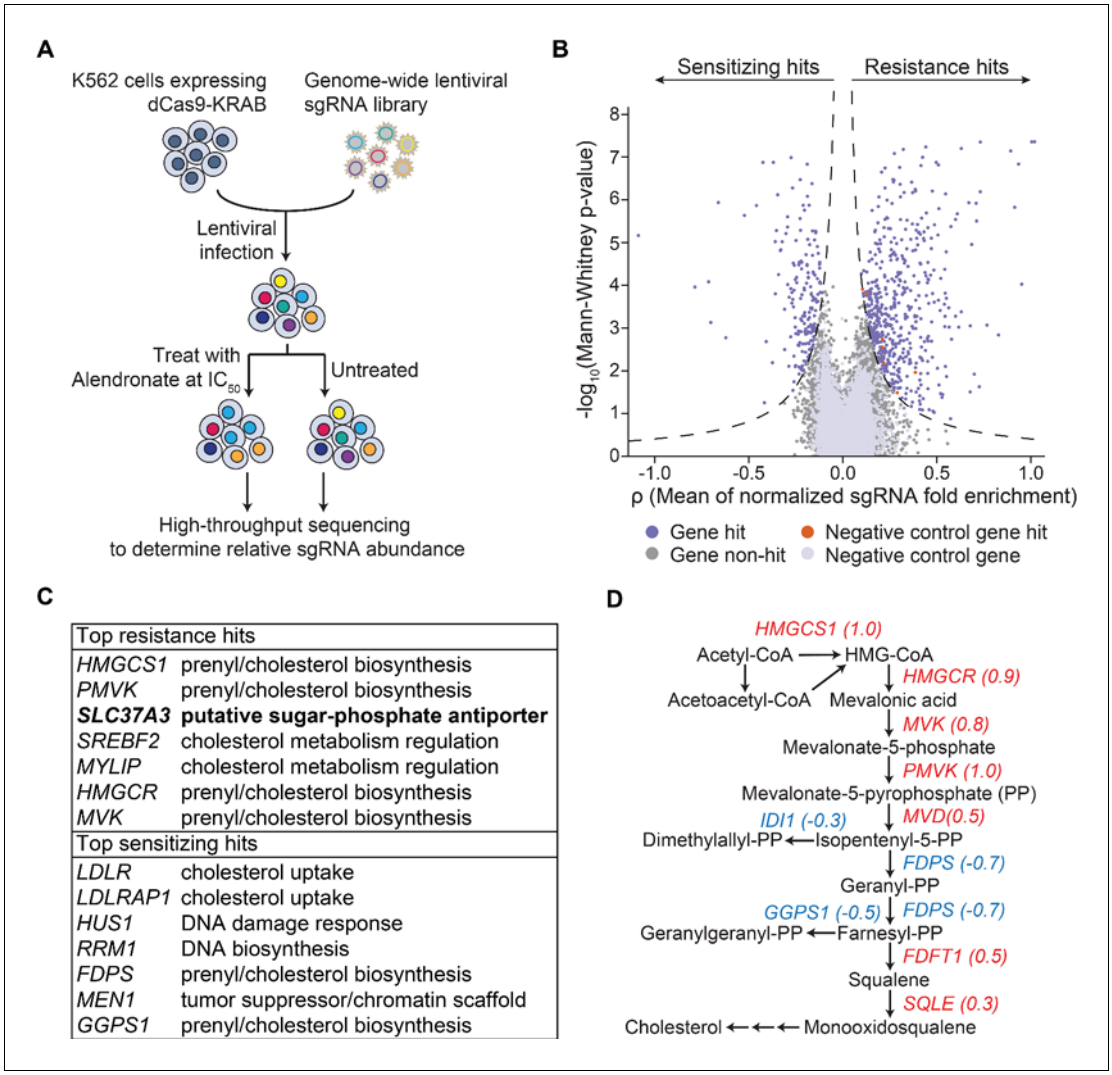

Figure 1. An unbiased CRISPRi screen identifies genetic targets of alendronate. (**A**) Schematic illustrating the workflow of the genome-wide CRISPRi screen. The IC_{50} of alendronate in K562 cells is 250 µM. (**B**) Volcano plot showing, for each gene, a ρ score that averages the normalized fold enrichment (in the treated population compared to the untreated control) of the gene's three most effective sgRNAs, and a Mann-Whitney *P*-value for fold enrichment (***Gilbert et al., 2014***). The dashed lines represent thresholds used to identify significant hits. Positive ρ scores correspond to resistance hits and negative scores to sensitizing hits. (**C**) Gene names and annotated functions of the top seven resistance and sensitizing hits. Genes are sorted by the absolute values of their ρ scores in descending order. *SLC37A3* is marked in bold. (**D**) Diagram of the mevalonate pathway, with genes in the pathway that were identified as significant hits marked with their ρ scores. Resistance hits are color-coded in red and sensitizing hits in blue.

DOI: https://doi.org/10.7554/eLife.36620.003

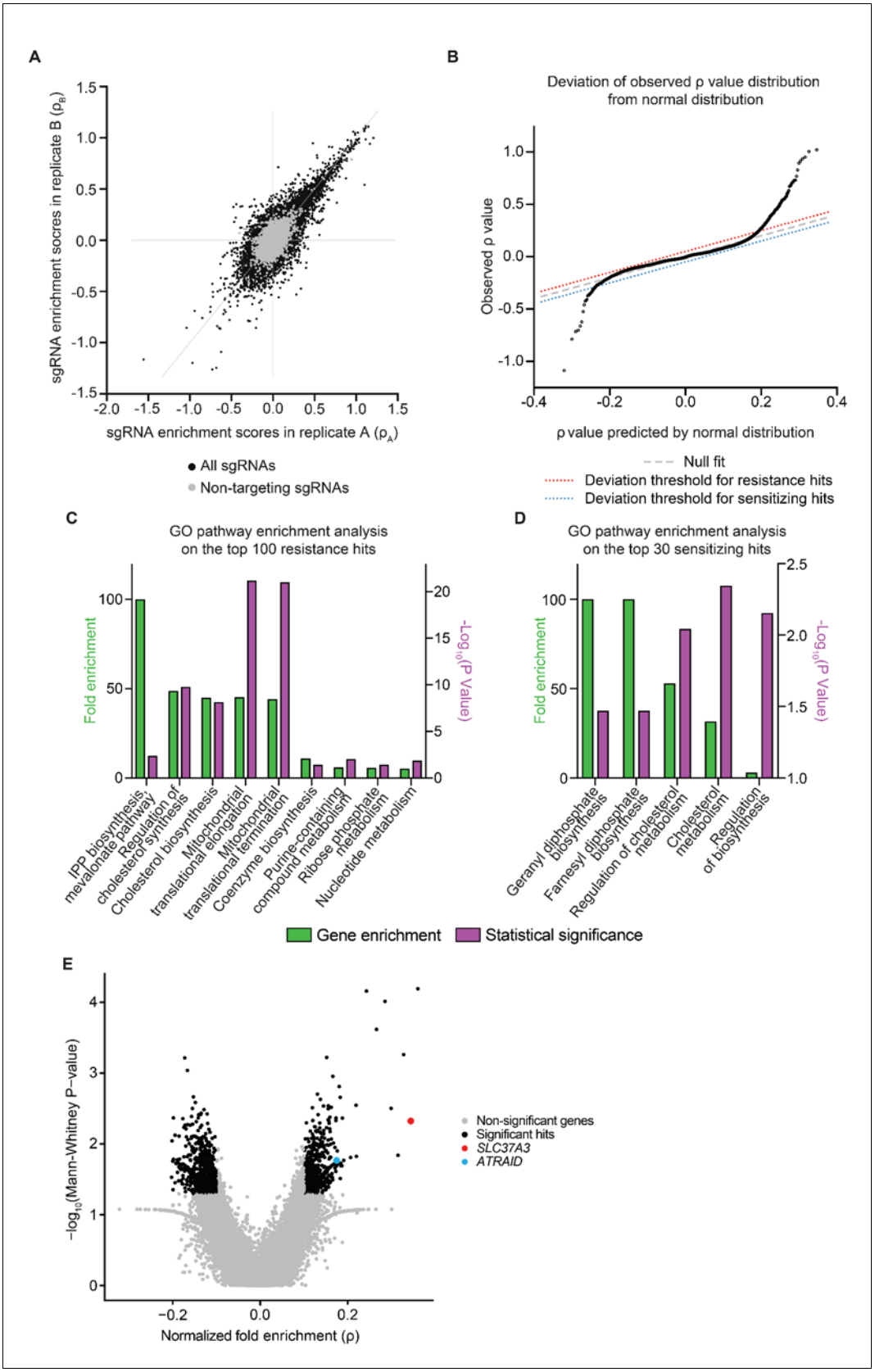

Figure 1—figure supplement 1. Additional analysis of the whole-genome CRISPRi screen. (**A**) Evaluation of the reproducibility of the CRISPRi screen. The enrichment score (ρ) of each sgRNA was calculated separately from two biological replicates of the CRISPRi screen and compared in a scatter plot.

Figure 1—figure supplement 1 continued on next page

Figure 1—figure supplement 1 continued

Data points corresponding to negative control sgRNAs are colored in gray. (**B**) Quantile-quantile plot comparing the distribution of observed average sgRNA enrichment scores (ρ scores) of each gene in the genome with a Gaussian distribution that has the same mean and standard deviation. The dashed gray line represents the predicted location of data points if the distribution of ρ scores is indeed Gaussian. The large deviations from the gray line observed at the two ends of the distribution indicate that the silencing of those genes has stronger effects than expected by pure Gaussian noise and is therefore likely to be biologically meaningful. The dotted lines are arbitrary thresholds set to select resistance hits (red dotted line) and sensitizing hits (blue dotted line) that deviate significantly from Gaussian predictions. 398 resistance hits and 28 sensitizing hits passed the thresholds. (**C–D**) Gene Ontology (GO) pathway enrichment analysis of the top 100 resistance hits (**C**) and the top 30 sensitizing hits (**D**) identified in the CRISPRi screen. Only the most specific subclasses that are statistically significant are shown. Both fold enrichment of pathway genes and *P*-values of fold enrichment are displayed. Fold enrichment values were clipped at 100 fold. *P*-values were corrected for multiple testing using Bonferroni correction. Note that genes involved in the mevalonate pathway, which includes IPP biosynthesis, geranyl phosphate synthesis and farnesyl phosphate synthesis, are significantly enriched in top hits from the screen. IPP: isopentenyl pyrophosphate. (**E**) Volcano plot showing the results from a second CRISPRi screen using zoledronate, another representative N-BP, as the selection agent. Plot layout is the same as in ***Figure 1B***. *SLC37A3* and *ATRAID* are highlighted in red and cyan, respectively. Significant hits were defined as genes that had a fold enrichment with an absolute value larger than 0.1, and a P-value smaller than 0.05.

DOI: https://doi.org/10.7554/eLife.36620.004

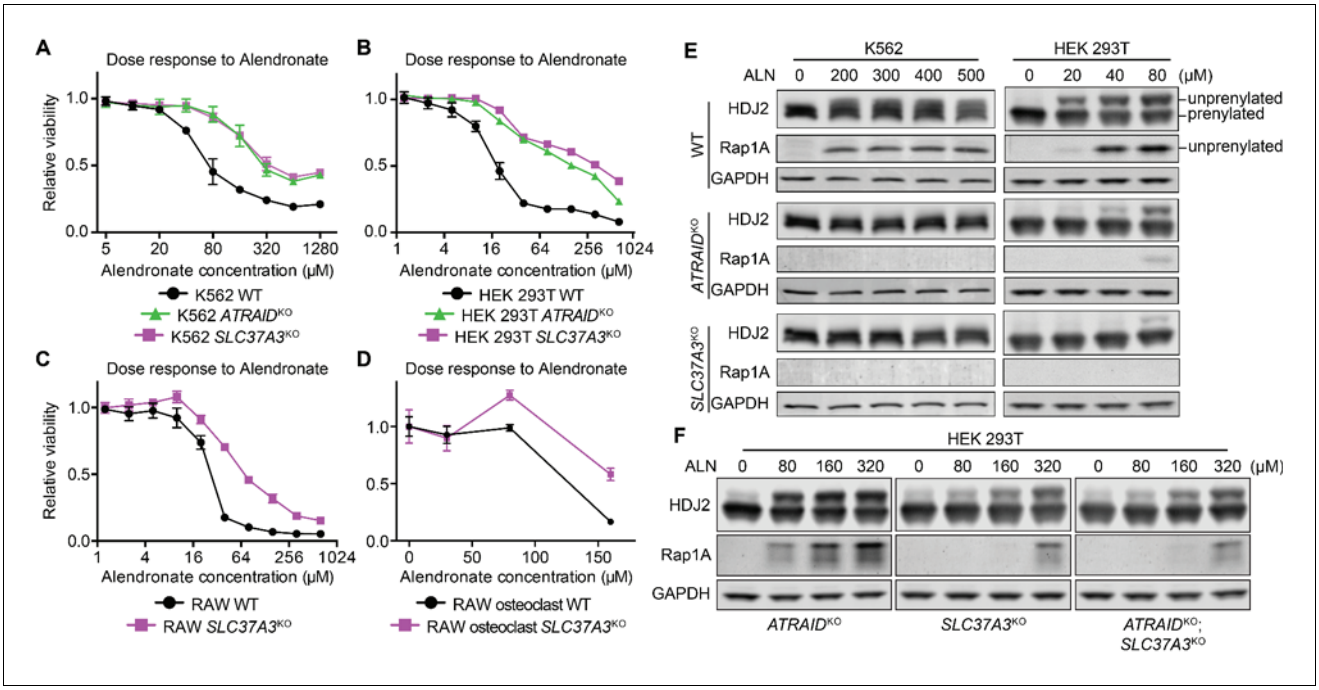

Figure 2. *SLC37A3* and *ATRAID* are functionally related genes required for the mechanism of action of N-BPs. (**A–D**) Dose response curves of wild-type, *ATRAID*^{KO} and *SLC37A3*^{KO} K562 cells (**A**) and HEK 293 T cells (**B**), and wild-type and *SLC37A3*^{KO} RAW cells (both undifferentiated macrophages, (**C**), and differentiated osteoclasts, (**D**) to alendronate. Cells were treated with a series of doses of alendronate (x-axis) for 48 hr. Relative cell viability was determined by measuring post-treatment total cellular ATP levels and normalizing to those in untreated cells (y-axis). Data depict mean with s.d. for biological triplicate measurements. (**E**) Immunoblots measuring alendronate-induced reduction in protein prenylation in wild-type and knockout K562 and HEK 293 T cells. Cells were treated with indicated doses of alendronate for 24 hr before analysis by immunoblotting. (**F**) Immunoblots comparing alendronate-induced reduction in protein prenylation in single and double-knockout HEK 293 T cells. Experimental procedure is as in (**C**). Note that higher alendronate doses were used in (**F**) compared to (**E**) to induce detectable levels of unprenylated proteins. ALN: alendronate.
DOI: https://doi.org/10.7554/eLife.36620.005

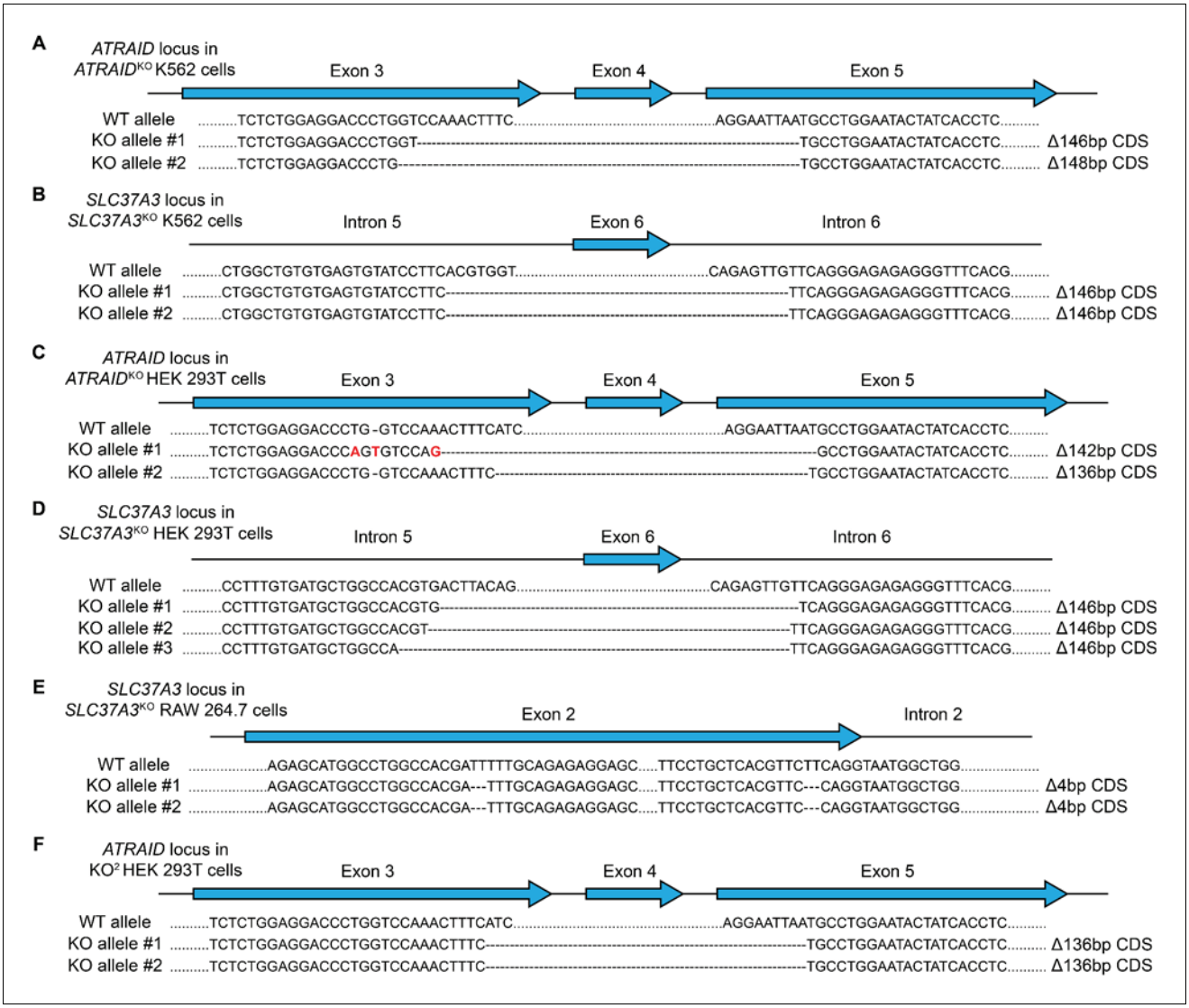

Figure 2—figure supplement 1. Genotypes of knockout cells used in this study. (**A–F**) Sequences of the *ATRAID* (**A, C and F**) or *SLC37A3* locus (**B, D and E**) in *ATRAID*^{KO} (**A**) and *SLC37A3*^{KO} (**B**) K562 cells, *ATRAID*^{KO} (**C**), *SLC37A3*^{KO} (**D**) and KO^{2} (**F**) HEK 293 T cells, and *SLC37A3*^{KO} (**E**) RAW 264.7 cells, showing that truncations in *ATRAID* and *SLC37A3* coding sequences (CDS) have caused frame shifts in the knockout cell lines. The *SLC37A3* locus in KO^{2} HEK 293 T cells is identical to that in *SLC37A3*^{KO} HEK 293 T cells. Introns and exons are not drawn to scale. Note that more than two alleles are present for the *SLC37A3* locus in HEK 293 T cells as these cells are hypo-triploidic. KO^{2}: *ATRAID*^{KO}; *SLC37A3*^{KO}.

DOI: https://doi.org/10.7554/eLife.36620.006

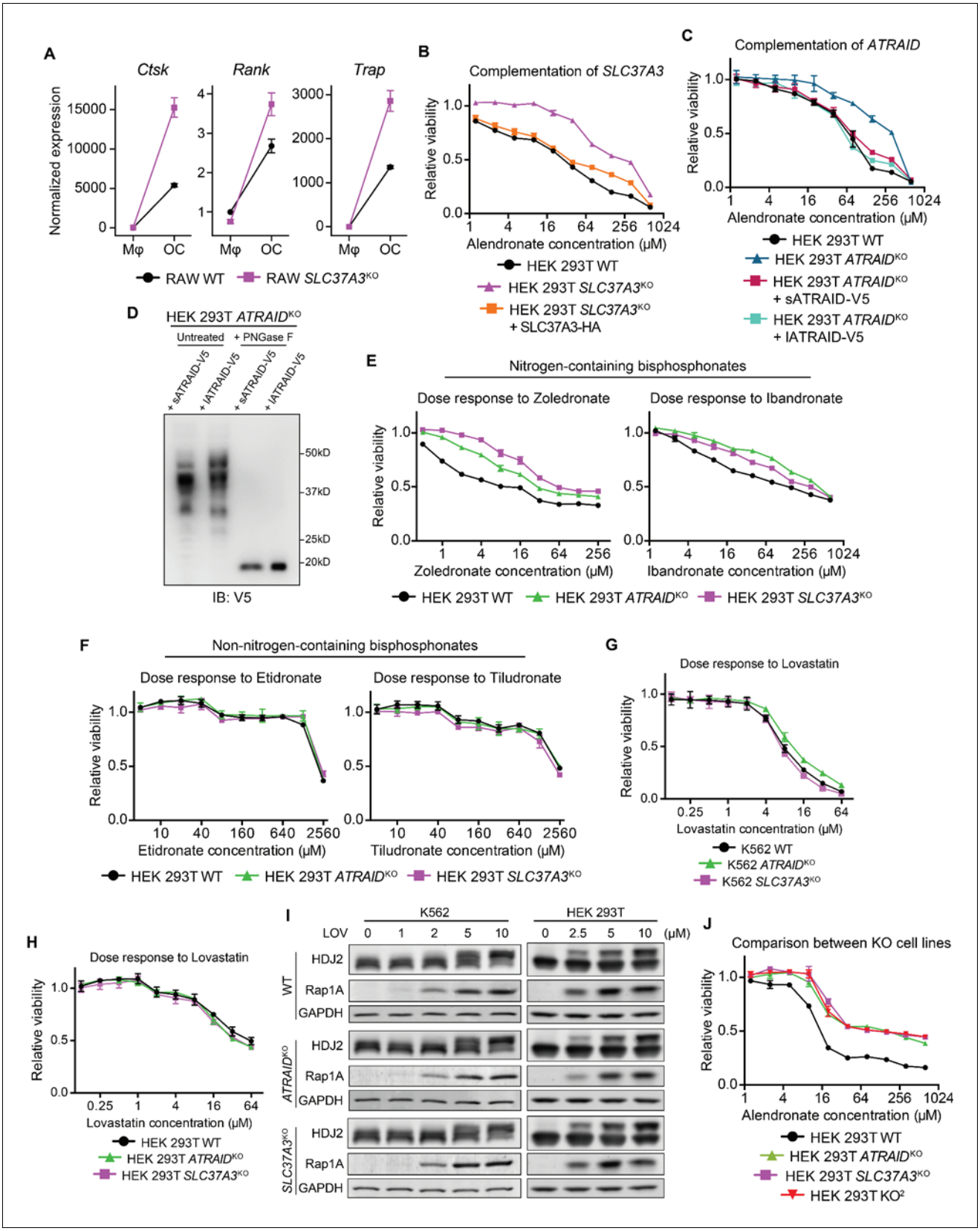

Figure 2—figure supplement 2. Additional evidence that validates *SLC37A3* and *ATRAID* as functionally related genes required for the mechanism of action of N-BPs. (**A**) Expression of osteoclast markers (*Ctsk, Rank* and *Trap*) in undifferentiated RAW macrophages (Mφ) and differentiated RAW

Figure 2—figure supplement 2 continued on next page

Figure 2—figure supplement 2 continued

osteoclasts (OC), demonstrating successful differentiation of RAW cells. (**B–C**) Dose responses to alendronate in *SLC37A3*^{KO} or *ATRAID*^{KO} HEK 293 T cells complemented with epitope tagged SLC37A3 or ATRAID, respectively, compared with those in wild-type, *ATRAID*^{KO} and *SLC37A3*^{KO} cells. (**D**) Immunoblot comparing the short isoform of ATRAID (sATRAID) with the long isoform of ATRAID (lATRAID), showing that the long isoform of ATRAID is expressed as the same protein as the short isoform of ATRAID. Note that unequal amount of protein was loaded in each lane to obtain even exposure. The amount of protein loaded from left to right was: 100 μg, 40 μg, 10 μg and 4 μg, respectively. (**E–F**) Dose response curves of wild-type, *ATRAID*^{KO} and *SLC37A3*^{KO} HEK 293 T cells to nitrogen-containing bisphosphonates (**E**) and non-nitrogen-containing bisphosphonates (**F**). (**G–H**) Dose response curves of wild-type, *ATRAID*^{KO} and *SLC37A3*^{KO} K562 cells (**G**) and HEK 293 T cells (**H**) to lovastatin. (**I**) Immunoblots measuring lovastatin-induced reduction in protein prenylation in wild-type, *ATRAID*^{KO} and *SLC37A3*^{KO} K562 cells and HEK 293 T cells. (**J**) Dose response to alendronate in KO^{2} HEK 293 T cells, compared with those in wild-type, *ATRAID*^{KO} and *SLC37A3*^{KO} cells. For (**B–C**), (**E–H**) and (**J**), data depict mean with s.d. for biological triplicate measurements. LOV: lovastatin. KO^{2}: *ATRAID*^{KO}; *SLC37A3*^{KO}. PNGase F: peptide: N-glycosidase F, an enzyme that removes asparagine (**N**)-linked sugar modifications on glycoproteins.

DOI: https://doi.org/10.7554/eLife.36620.007

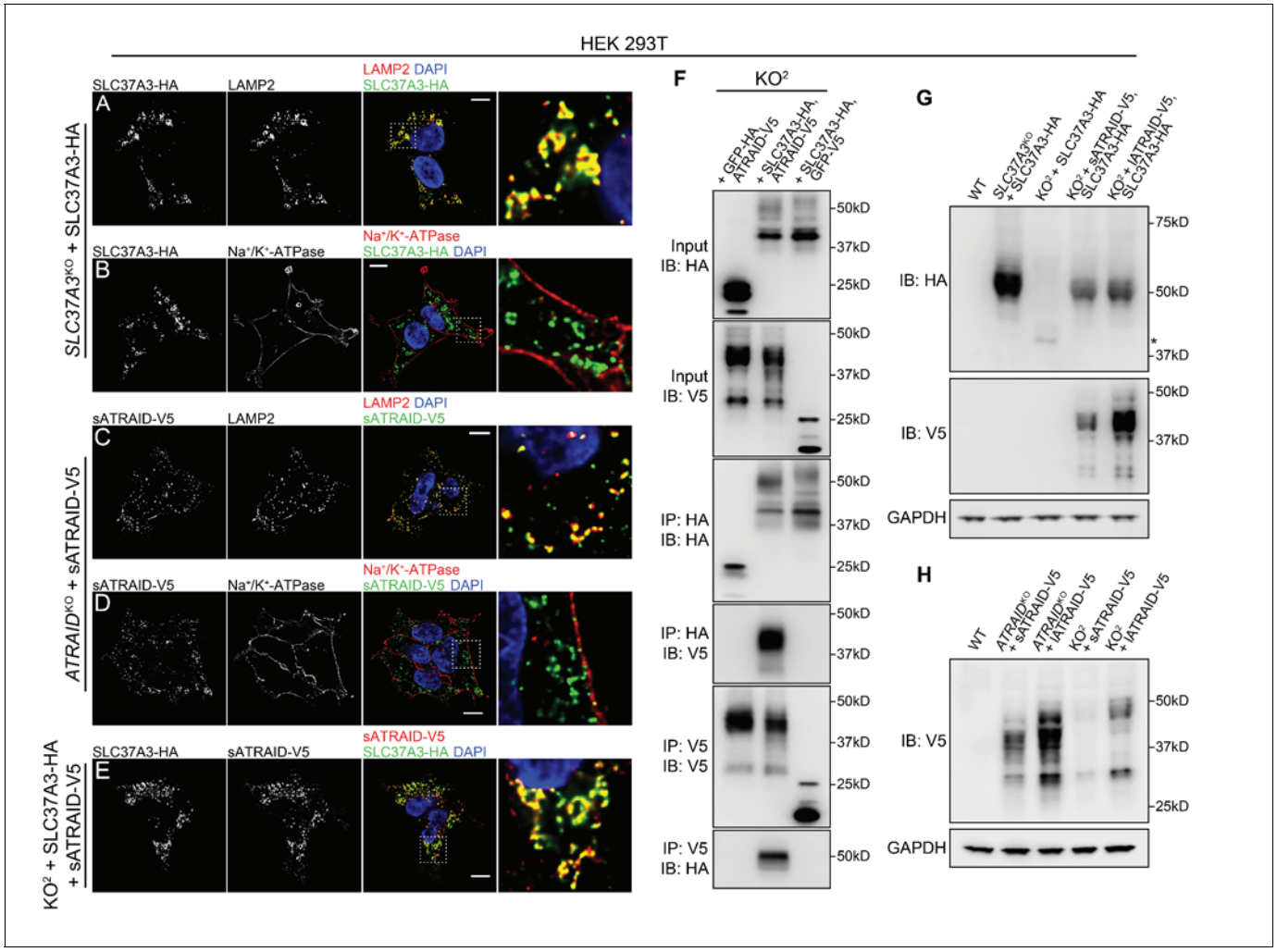

Figure 3. SLC37A3 and ATRAID form a lysosomal complex and are inter-dependent for their stable expression. (**A–D**) Localization of HA-tagged SLC37A3 (SLC37A3-HA) (**A–B**) and V5-tagged short isoform of ATRAID (sATRAID-V5) (**C–D**) shown with markers for lysosomes (LAMP2, (**A and C**) and the plasma membrane (Na^+/K^+-ATPase, (**B and D**). (**E**) Co-localization of SLC37A3-HA and sATRAID-V5. Nuclei were stained with DAPI in blue. Scale bars represent 10 μm. Each image displayed is the representative example chosen from at least five similar images. (**F**) Reciprocal co-IP of SLC37A3A3-HA and sATRAID-V5 in KO^2 HEK 293 T cells stably overexpressing both proteins. In each negative control cell line, one of the two tagged proteins was replaced with GFP tagged with the same epitope. (**G**) Immunoblots measuring SLC37A3-HA protein levels in various cells, showing that deletion of *ATRAID* significantly reduces the protein level of SLC37A3-HA. The un-glycosylated population of SLC37A3 that appears in the absence of ATRAID is marked with an asterisk. (**H**) Immunoblots measuring ATRAID-V5 protein levels in various cells, demonstrating that deletion of *SLC37A3* significantly reduces the protein level of ATRAID-V5. IP, immunoprecipitation. IB, immunoblot. KO^2: $ATRAID^{KO}$; $SLC37A3^{KO}$.

DOI: https://doi.org/10.7554/eLife.36620.008

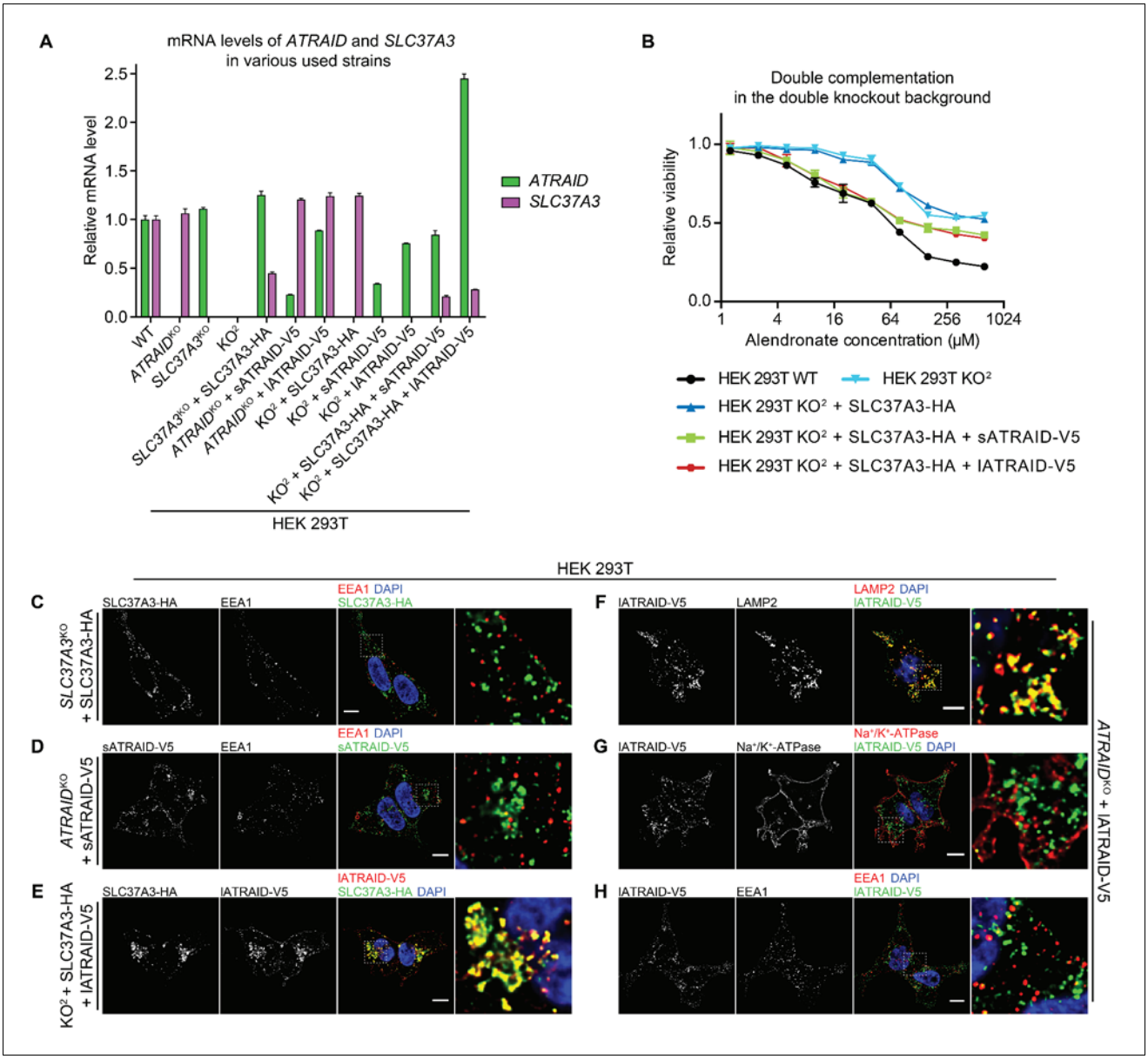

Figure 3—figure supplement 1. Additional evidence supporting that SLC37A3 and ATRAID form a lysosomal complex. (**A**) mRNA levels of *ATRAID* and *SLC37A3* in various HEK 293 T cells used in this study. Data depict mean and s.d. for technical triplicate measurements. (**B**) Dose responses to alendronate in KO^2 HEK 293 T cells complemented with either only SLC37A3-HA or both ATRAID-V5 and SLC37A3-HA, compared with those in wild-type and KO^2 HEK 293 T cells. Data depict mean and s.d. for biological triplicate measurements. (**C–H**) Localization of SLC37A3-HA (**C**), sATRAID-V5 (**D**) or lATRAID-V5 (**F–H**) shown with LAMP2 (**F**), EEA1 (**C, D and H**) and Na^+/K^+-ATPase (**G**), and co-localization of SLC37A3-HA and lATRAID-V5 (**E**). Scale bars represent 10 μm. Each image displayed is the representative example chosen from at least five similar images. Note that in **E**), there exists a subpopulation of lATRAID-V5 that localizes to the plasma membrane but not with SLC37A3-HA. Such distribution is likely a result of a higher-than-endogenous expression level of lATRAID-V5 in KO^2 +SLC37A3-HA + lATRAID-V5 HEK 293 T cells (**A**), as such distribution is not observed in $ATRAID^{KO}$ +lATRAID-V5 HEK 293 T cells (**G**), which express lATRAID-V5 at a lower-than-endogenous level (**A**). KO^2: $ATRAID^{KO}$; $SLC37A3^{KO}$. sATRAID: short isoform of ATRAID. lATRAID: long isoform of ATRAID.

DOI: https://doi.org/10.7554/eLife.36620.009

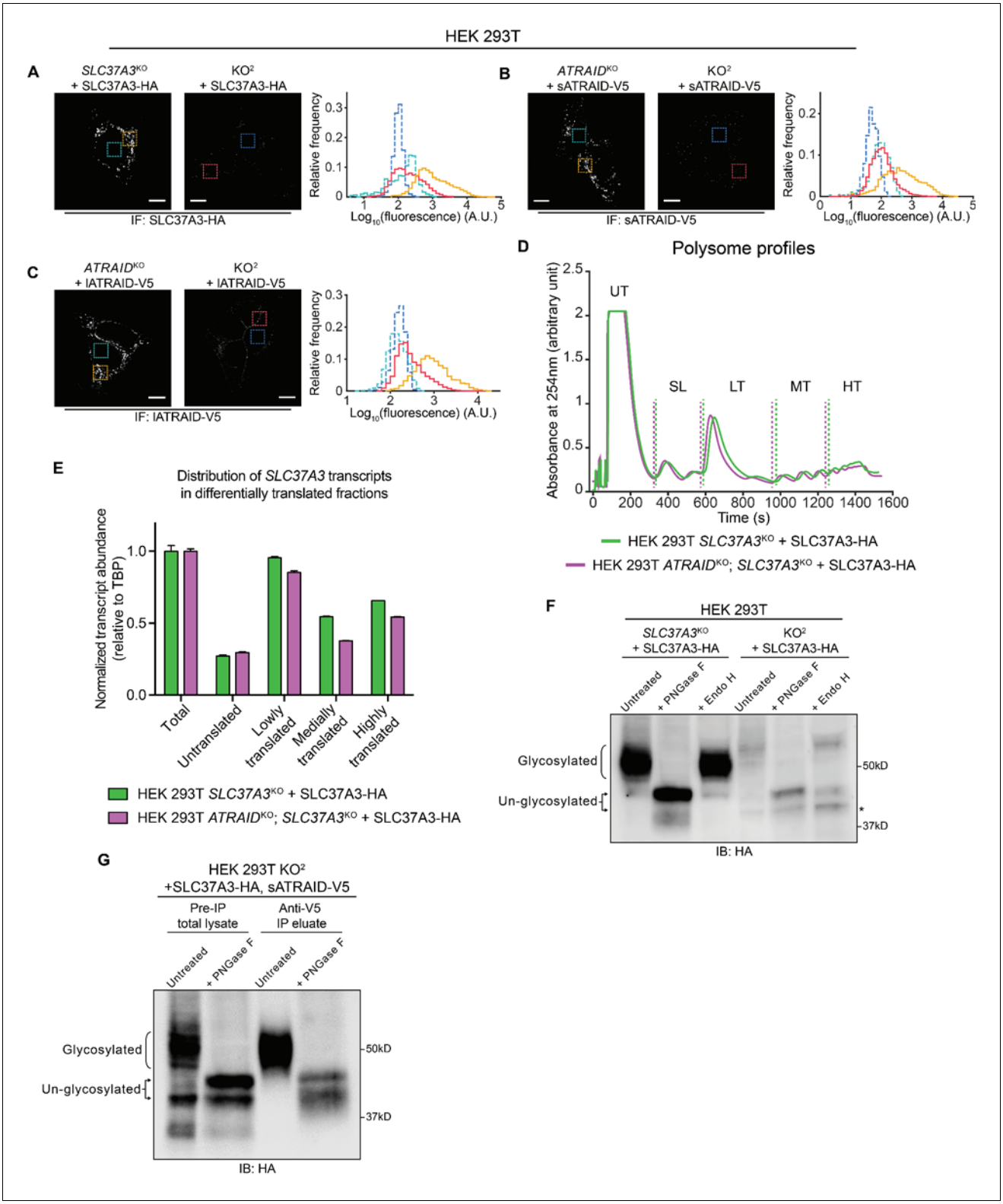

Figure 3—figure supplement 2. Additional evidence supporting that SLC37A3 and ATRAID depend on each other for stable expression. (**A–C**) Analysis of IF images comparing the expression levels of SLC37A3-HA (**A**) or both isoforms of ATRAID-V5 (**B and C**) in their respective single knockout backgrounds and the KO^2 background. The two images in each sub-figure were acquired with the same setting and adjusted to the same contrast. In each image a background area (turquoise or blue, inside nuclei, where no stain should be present) and a signal area (orange or red) were selected and the distribution of pixel values within each area was plotted in a histogram. The outlines in the histogram are color-coded to match the boarders of

Figure 3—figure supplement 2 continued on next page

Figure 3—figure supplement 2 continued

selected areas. (**D–E**) Polysome profiling experiment assessing the translation efficiency of *SLC37A3* transcripts in *SLC37A3*^{KO} and KO^{2} backgrounds. Lysates from indicated cell lines were analyzed on a gradient station and fractionated into five fractions: untranslated transcripts (UT), small and large ribosome subunits (SL), lowly translated transcripts (LT), medially translated transcripts (MT) and highly translated transcripts (HT). The level of *SLC37A3* transcripts relative to the level of *TBP* (TATA-binding protein) transcripts in each fraction was measured and plotted. The SL fraction was excluded from the analysis. A total RNA fraction was included as a reference. No overall shift was observed in the distribution of *SLC37A3* transcripts in the KO^{2} background compared to that in the *SLC37A3*^{KO} background, suggesting that the translation efficiency of *SLC37A3* is not affected by the absence of *ATRAID*. (**F**) Immunoblot comparing the glycosylation patterns of SLC37A3 in *SLC37A3*^{KO} and KO^{2} backgrounds. Lysates from *SLC37A3*^{KO} + SLC37A3-HA (lane 1–3) and KO^{2} + SLC37A3-HA (lane 4–6) HEK 293 T cells were left untreated (lane 1 and 4), treated with PNGase-F (lane 2 and 5), or with Endo H (lane 3 and 6). The band corresponding to an un-glycosylated population of SLC37A3 that is present in the absence of ATRAID but not in the presence of ATRAID is marked with an asterisk. (**G**) Immunoblot comparing the glycosylation patterns of total cellular SLC37A3 and the sub-population of SLC37A3 that interacts with ATRAID. In KO^{2} HEK 293 T cells over-expressing SLC37A3-HA and sATRAID-V5, proteins that interact with sATRAID-V5 were purified with immuno-precipitation against V5 epitope and compared with total proteins in the lysate. The pre-IP total lysate (lane 1–2) and anti-V5 IP eluate (lane 3–4) were either left untreated (lane 1 and 3) or treated with PNGase F (lane 2 and 4) and analyzed by blotting against SLC37A3-HA. IF: immunofluorescence. IB: immunoblot. KO^{2}: *ATRAID*^{KO}; *SLC37A3*^{KO}. PNGase F: peptide: N-glycosidase F, an enzyme that removes all asparagine (**N**)-linked sugar modifications from glycoproteins. Endo H: endoglycosidase H, an enzyme that only removes high mannose sugar moieties on ER glycoproteins that have not been processed by the Golgi apparatus.

DOI: https://doi.org/10.7554/eLife.36620.010

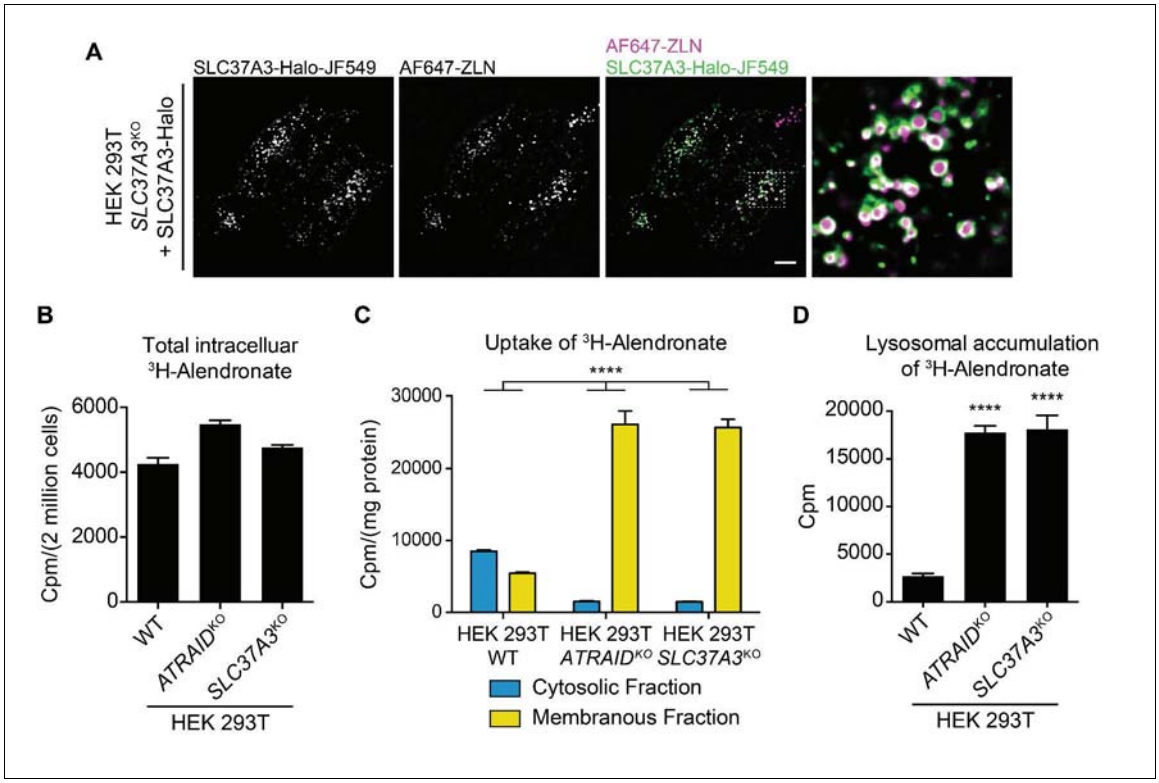

Figure 4. SLC37A3 and ATRAID transport N-BPs from the lumen of lysosomes into the cytosol. (**A**) Live imaging of HEK 293 T cells that express Halo tagged SLC37A3 (SLC37A3-Halo) and have internalized AlexaFlour 647 labeled zoledronate (AF647-ZLN). SLC37A3-Halo is labeled with Janelia flour 549 (JF549). SLC37A3-Halo is expressed at a lower-than-endogenous level and has been verified to be functional (data not shown). The scale bar represents 10 μm. The image displayed is a representative example chosen from five similar images. (**B**) Radioactive uptake assay measuring total intracellular radioactivity in indicated HEK 293 T cells treated with ^{3}H-alendronate. Data depict mean and s.d. for biological triplicate measurements. (**C**) Radioactive uptake assay measuring levels of radioactivity in subcellular fractions in indicated HEK 293 T cells treated with ^{3}H-alendronate. Data depict mean with s.d. for biological duplicate measurements. Significance was determined using unpaired two-way ANOVA test. Effect of genotype: $F(2,6) = 74.93$, $p<0.0001$; effect of subcellular location: $F(1,6) = 864.9$, $p<0.0001$; effect of interaction between genotype and subcellular location: $F(2,6) = 312.4$, $p<0.0001$. (**D**) Radioactive uptake assay measuring levels of radioactivity in lysosomes purified from indicated HEK 293 T cells treated with ^{3}H-alendronate. Data depict mean and s.d. for biological triplicate measurements. Significance was determined using two-tailed unpaired t-test with equal s.d. Comparison between wild-type and *ATRAID*^{KO} cells: df = 4, t = 36.24, $p<0.0001$. Comparison between wild-type and *SLC37A3*^{KO} cells: df = 4, t = 17.96, $p<0.0001$. HEK 293 T cells were treated with 1 μCi/mL ^{3}H-alendronate for 24 hr in (**B–C**) and 3 hr in (**D**). ****: $p<0.0001$.

DOI: https://doi.org/10.7554/eLife.36620.011

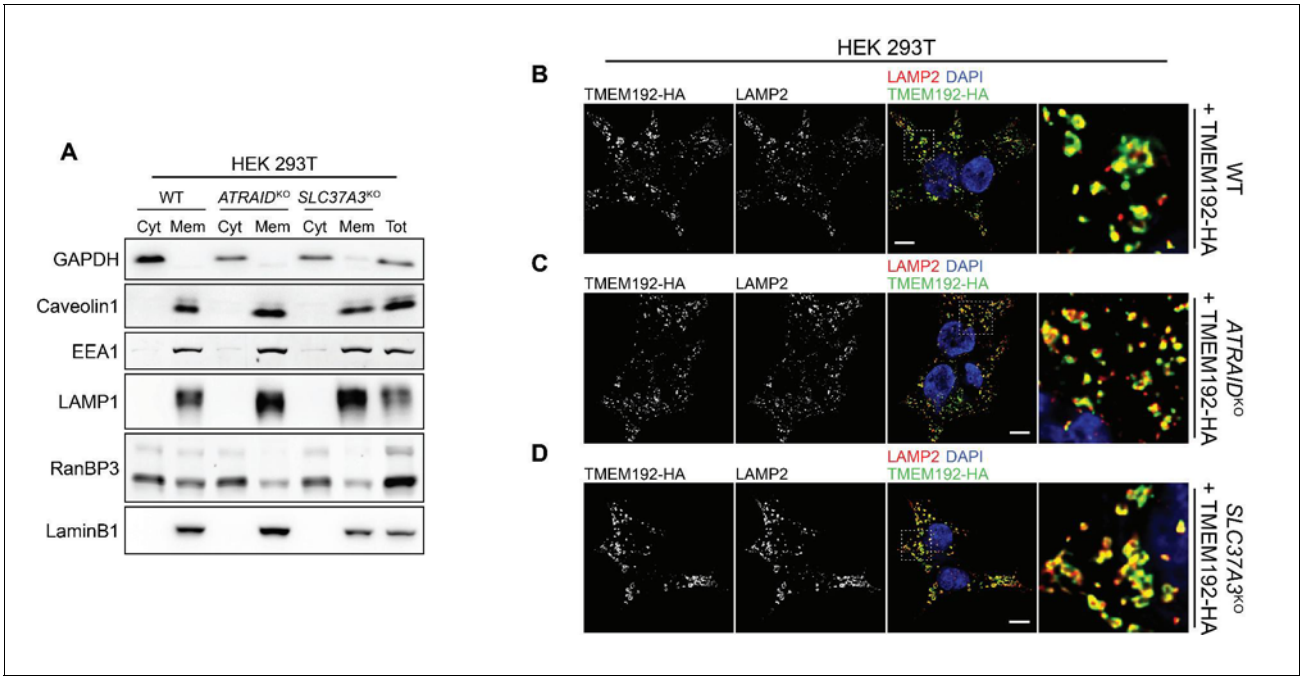

Figure 4—figure supplement 1. Quality controls for the radioactive uptake assays. (**A**) Immunoblot against markers for cytosol (GAPDH), plasma membrane (Caveolin1), early endosome (EEA1), lysosome (LAMP1), nucleosol (RaN-BP3), and nucleoskeleton (LaminB1) in cytosolic fractions and membranous fractions in wild-type, *ATRAID*^{KO} and *SLC37A3*^{KO} HEK 293 T cells, demonstrating successful subcellular fractionation in the fractionation-based radioactive uptake assay. Cyt: cytosolic fraction. Mem: membranous fraction. Tot: total cell lysate. (**B–D**) Localization of HA tagged TMEM192 (TMEM192-HA), a lysosomal protein we expressed in wild-type (**B**), *ATRAID*^{KO} (**C**) and *SLC37A3*^{KO} (**D**) HEK 293 T cells and used as a handle to immuno-precipitate lysosomes, shown with a lysosomal marker, LAMP2, demonstrating correct localization of TMEM192-HA to lysosomes and, consequently, successful purification of lysosomes in the lysosome-purification-based uptake assay. Scale bars represent 10 μm. Each image displayed is the representative example chosen from at least five similar images.

DOI: https://doi.org/10.7554/eLife.36620.012